catalysts

MDPI

Supplementary Materials

Tungsten Oxide Morphology-Dependent Au/TiO_2/WO_3 Heterostructures with Applications in Heterogenous Photocatalysis and Surface-Enhanced Raman Spectroscopy

István Székely [1,2,3], Zoltán Kovács [1,2,4], Mihai Rusu [2,5], Tamás Gyulavári [4], Milica Todea [2,6], Monica Focșan [7], Monica Baia [2,3,8,*] and Zsolt Pap [2,3,4,*]

1 Doctoral School of Physics, Babes-Bolyai University, M. Kogălniceanu 1, 400084 Cluj-Napoca, Romania; istvan.szekely@ubbcluj.ro (I.S.); zoltan.kovacs@ubbcluj.ro (Z.K.)
2 Centre of Nanostructured Materials and Bio-Nano Interfaces, Institute for Interdisciplinary Research on Bio-Nano-Sciences, Treboniu Laurian 42, 400271 Cluj-Napoca, Romania; mihai.rusu@phys.utcluj.ro (M.R.)
3 Laboratory for Advanced Materials and Applied Technologies, Institute for Research, Development and Innovation in Applied Natural Sciences, Fantanele 30, 400294 Cluj-Napoca, Romania
4 Department of Applied and Environmental Chemistry, University of Szeged, Rerrich Sqr. 1, HU-6720 Szeged, Hungary; gyulavarit@chem.u-szeged.hu
5 Department of Physics and Chemistry, Technical University of Cluj-Napoca, Memorandumului 28, 400114 Cluj-Napoca, Romania
6 Faculty of Medicine, Iuliu Haţieganu University of Medicine and Pharmacy, Victor Babeș 8, 400012 Cluj-Napoca, Romania
7 Nanobiophotonics and Laser Microspectroscopy Center, Interdisciplinary Research Institute on Bio-Nano-Sciences, Treboniu Laurian 42, Babes-Bolyai University, 400271 Cluj-Napoca, Romania; monica.iosin@ubbcluj.ro
8 Faculty of Physics, Babeș-Bolyai University, Mihail Kogălniceanu Str. 1, 400084 Cluj-Napoca, Romania
* Correspondence: monica.baia@ubbcluj.ro (M.B.); zsolt.pap@ubbcluj.ro (Z.P.)

Citation: Székely, I.; Kovács, Z.; Rusu, M.; Gyulavári, T.; Todea, M.; Focșan, M.; Baia, M.; Pap, Z. Tungsten Oxide Morphology-Dependent Au/TiO_2/WO_3 Heterostructures with Applications in Heterogenous Photocatalysis and Surface-Enhanced Raman Spectroscopy. *Catalysts* **2023**, *13*, x. https://doi.org/10.3390/xxxxx

Academic Editors: Detlef W. Bahnemann and Jorge Bedia

Received: 29 March 2023
Revised: 12 June 2023
Accepted: 15 June 2023
Published: date

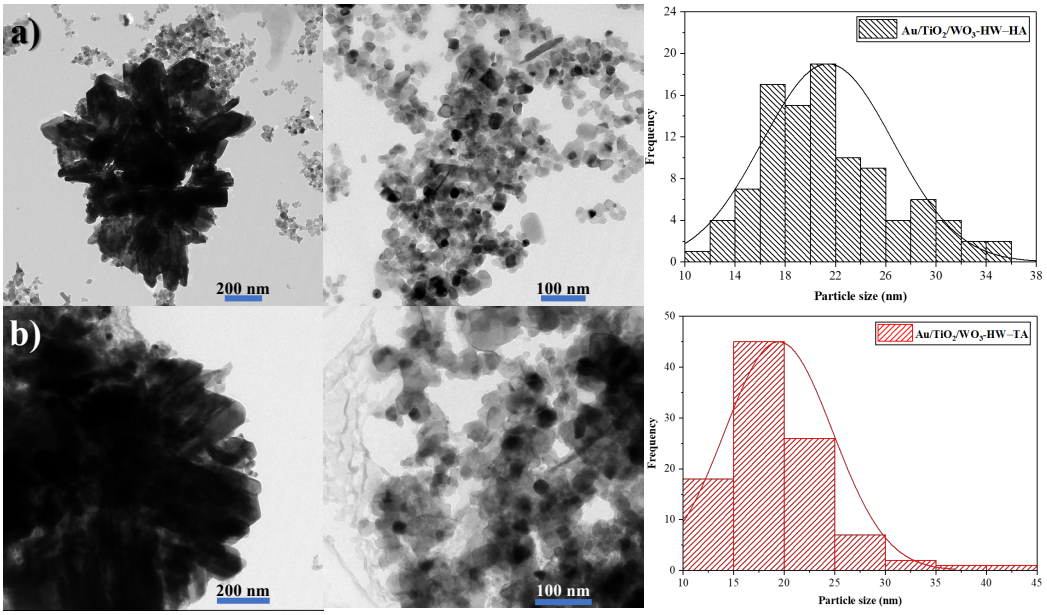

Figure S1. TEM micrographs of Au/TiO_2/WO_3-HW−HA (a) and Au/TiO_2/WO_3-HW−TA (b) samples, and their corresponding size distribution histograms for gold nanoparticles.

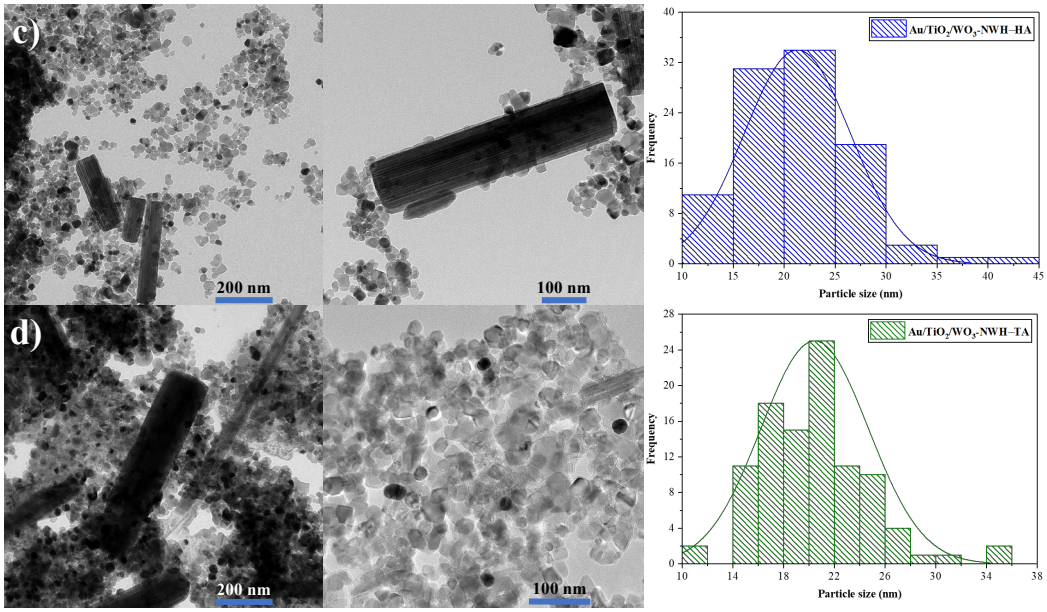

Figure S2. TEM micrographs of Au/TiO_2/WO_3-NWH−HA (c) and Au/TiO_2/WO_3-NWH−TA (d), and their corresponding size distribution histograms for gold nanoparticles.

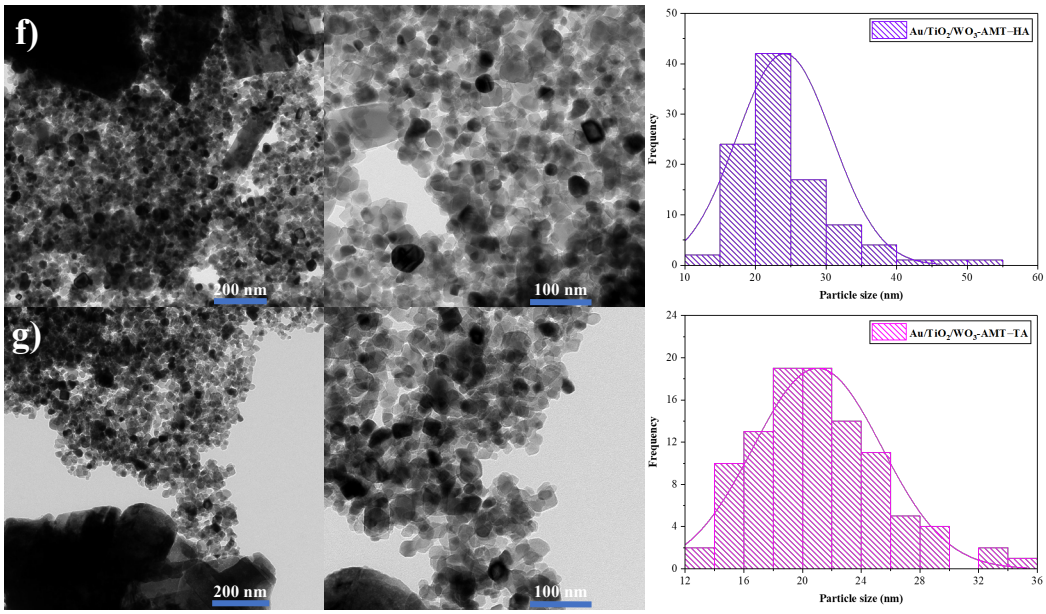

Figure S3. TEM micrographs of Au/TiO_2/WO_3-AMT−HA (f) and Au/TiO_2/WO_3-AMT−TA (g), and their corresponding size distribution histograms for gold nanoparticles.

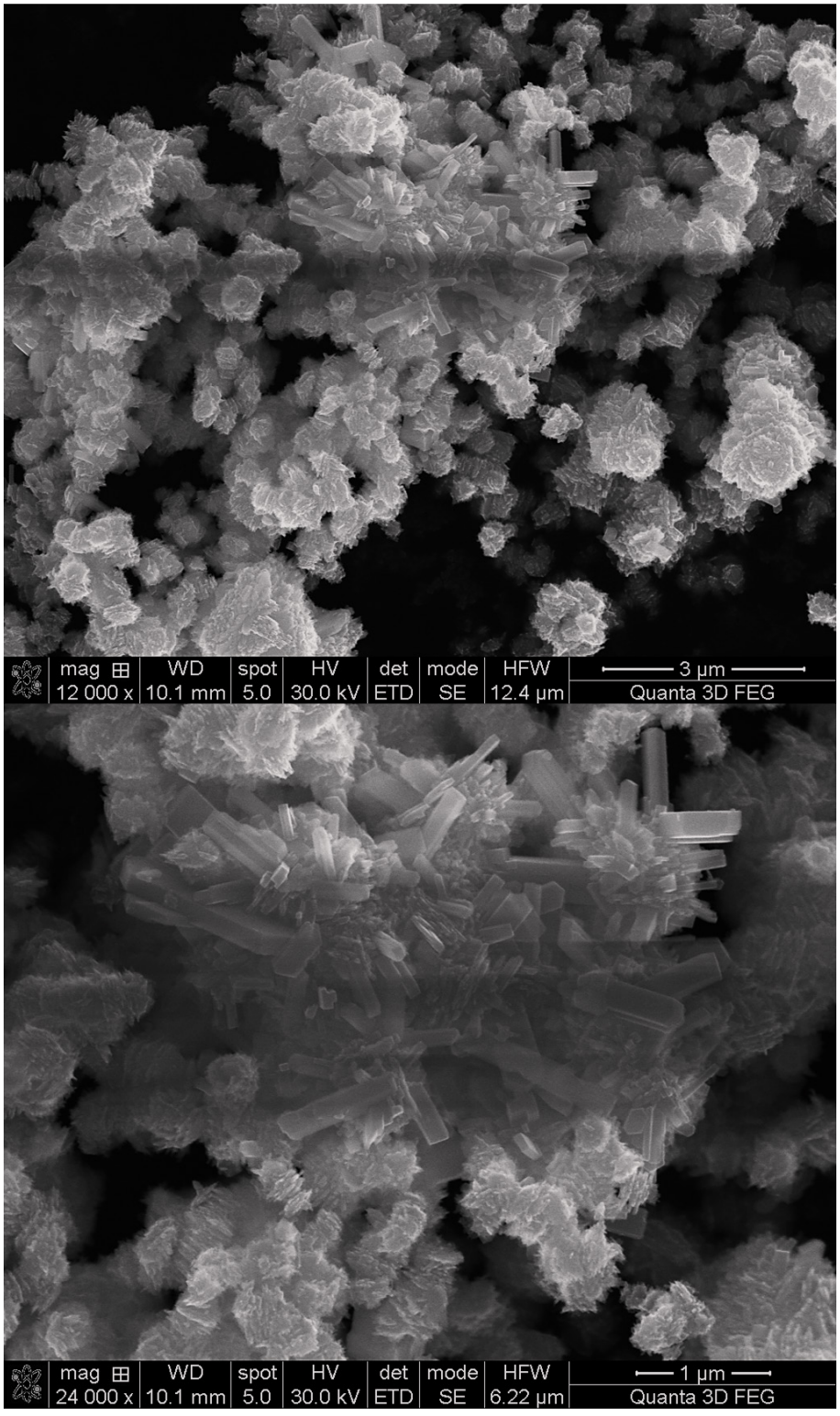

Figure S4. SEM micrographs of the prismatic dipyramid WO_3-HW semiconductors (3—1 µm).

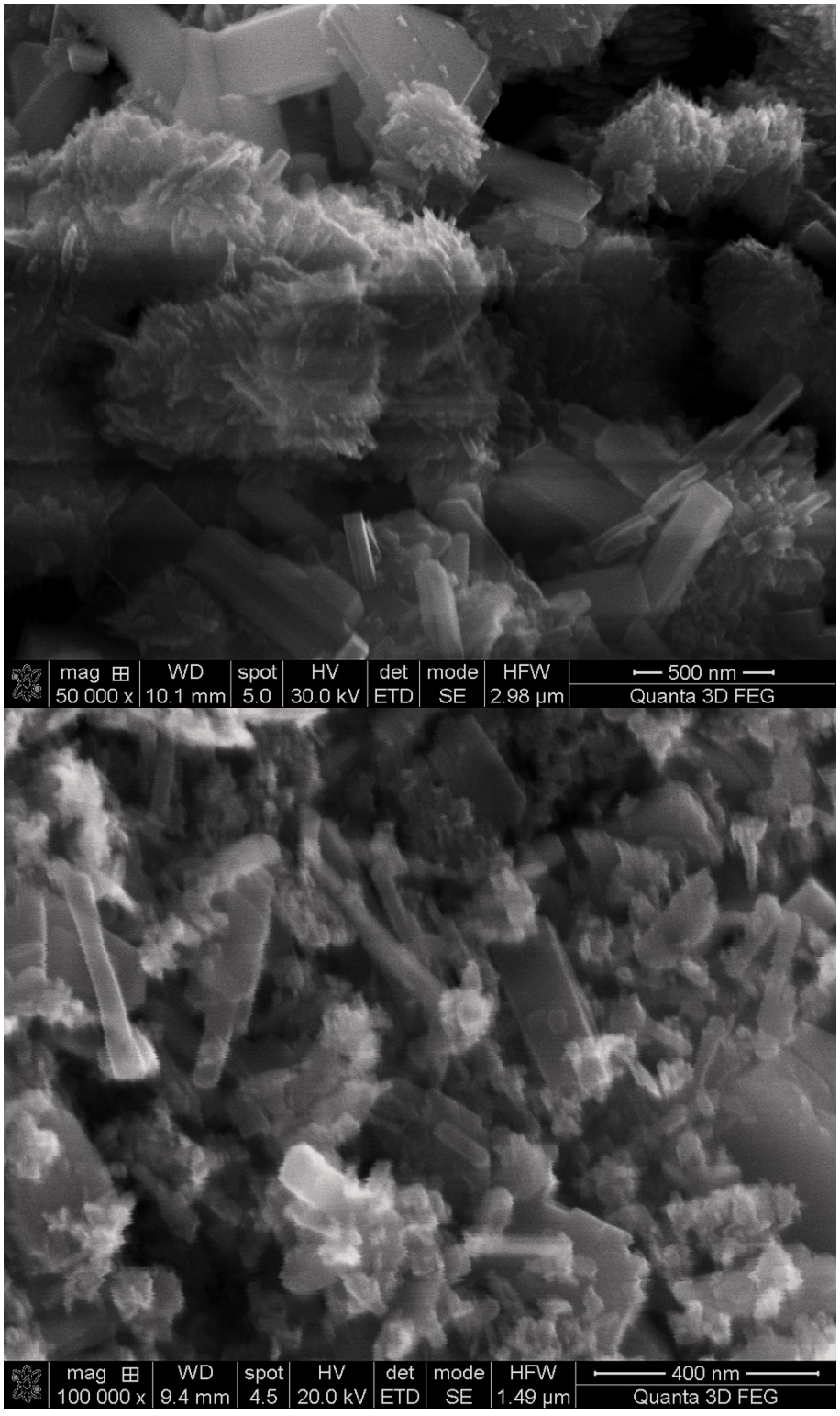

Figure S5. SEM micrographs of the prismatic dipyramid WO_3-HW semiconductors (500─400 nm).

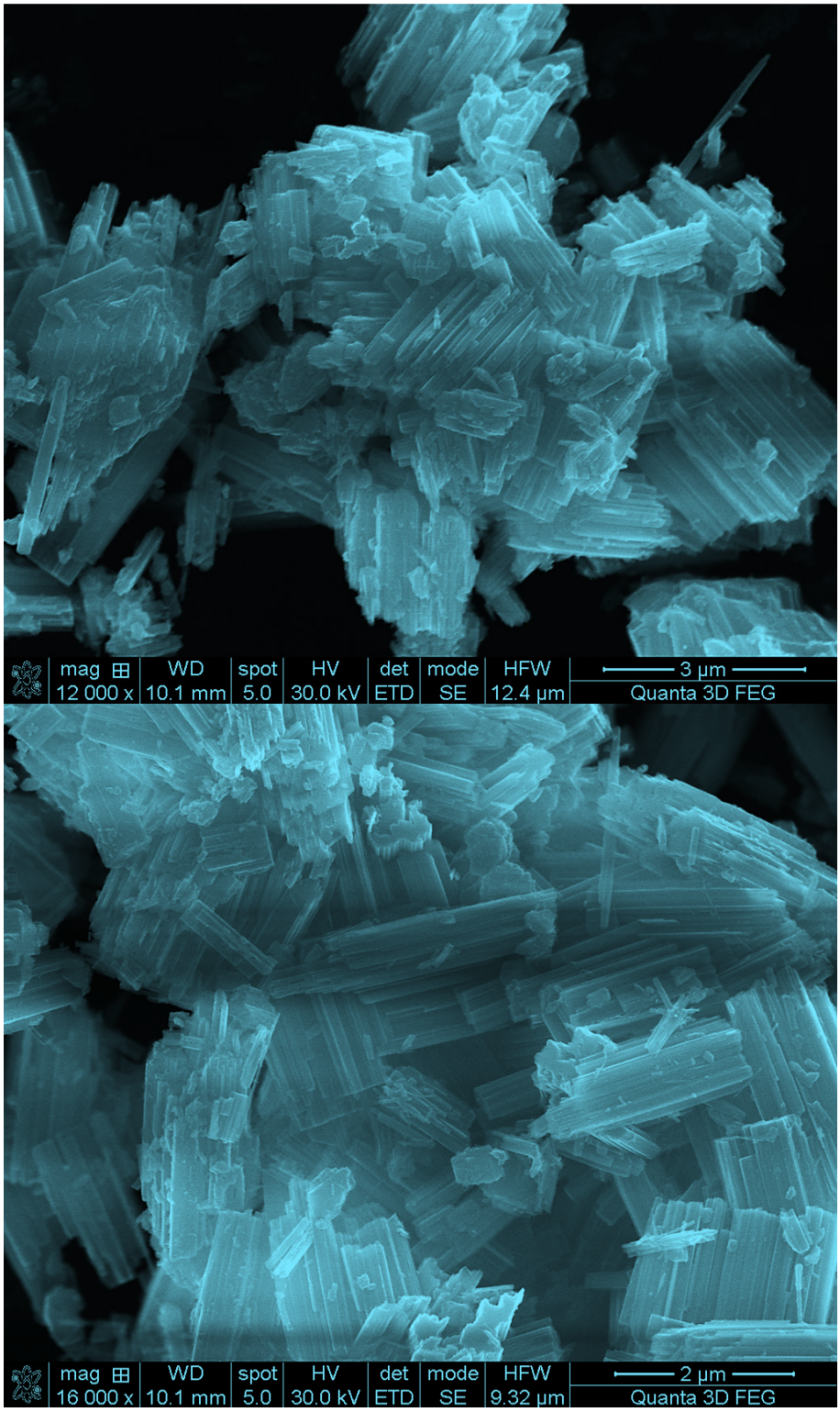

Figure S6. SEM micrographs of the rod-like/wire-like WO_3-NWH semiconductors (3─2 µm).

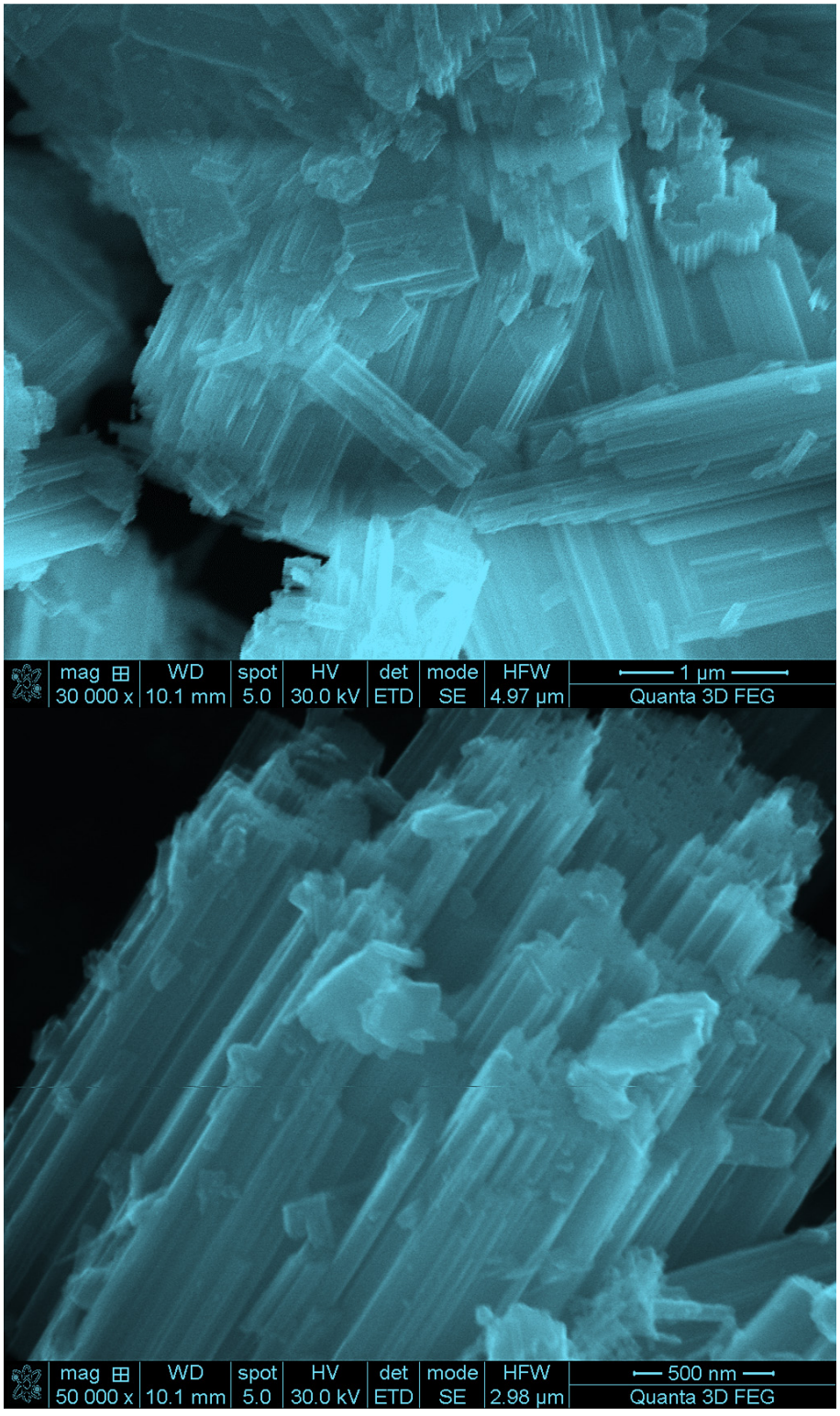

Figure S7. SEM micrographs of the rod-like/wire-like WO_3-NWH semiconductors (1─0.5 µm).

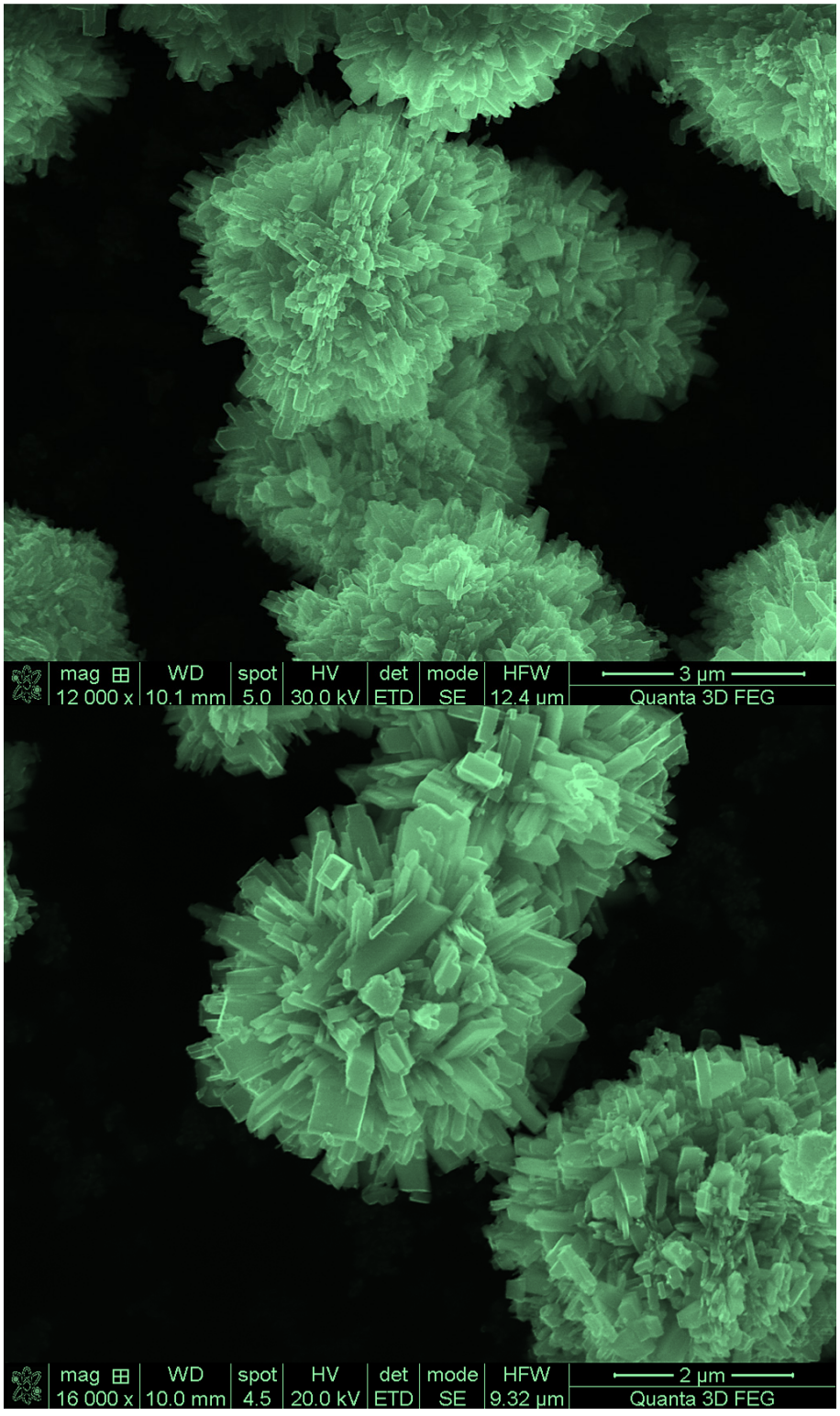

Figure S8. SEM micrographs of the flower-like WO_3-AMT semiconductors (3─2 µm).

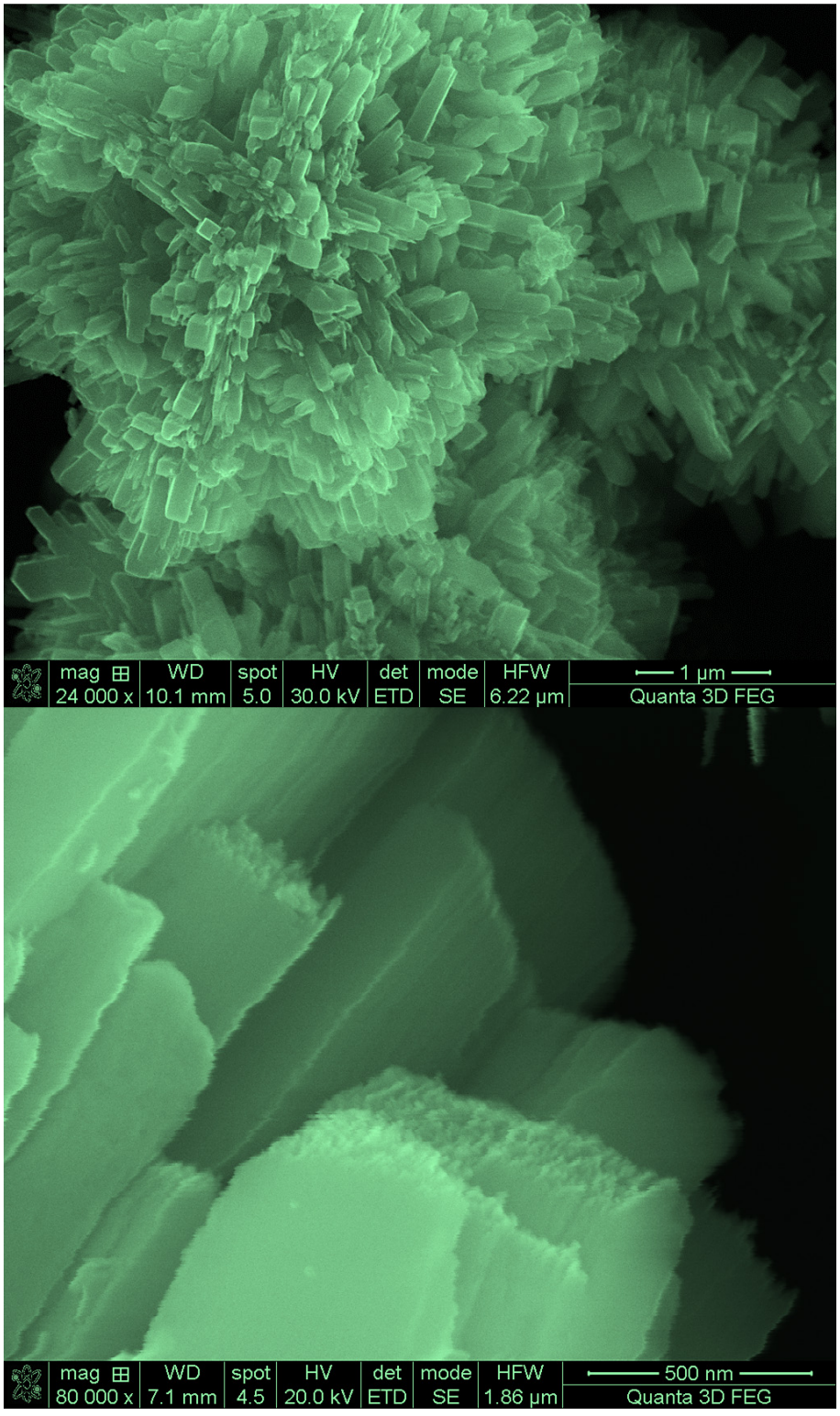

Figure S9. SEM micrographs of the flower-like WO_3-AMT semiconductors (1─0.5 µm).

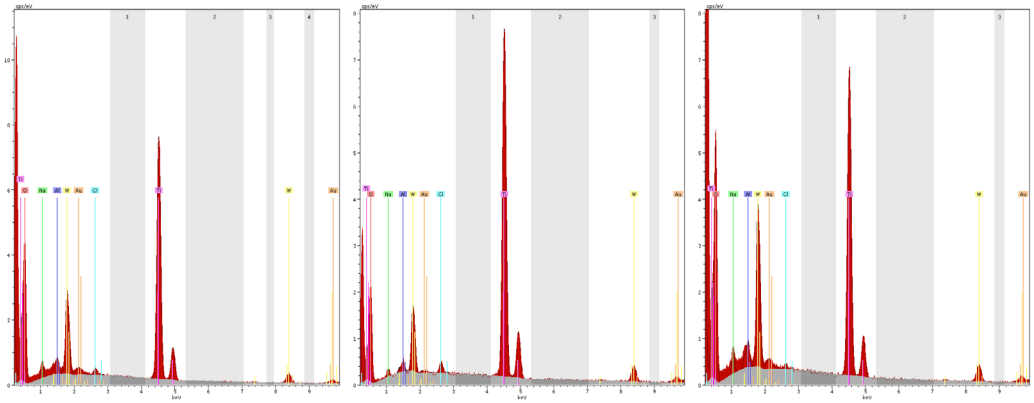

Figure S10. SEM-EDX spectra of the Au/TiO_2/WO_3-HW—HA heterostructures.

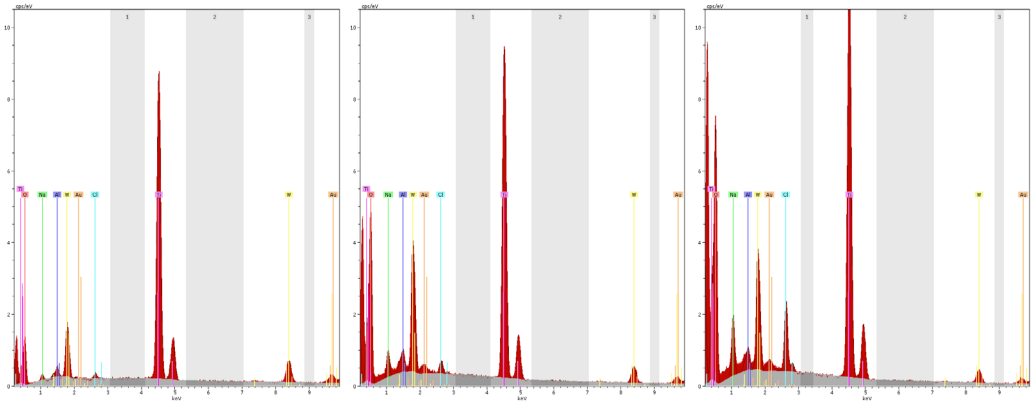

Figure S11. SEM-EDX spectra of the Au/TiO_2/WO_3-HW—TA heterostructures.

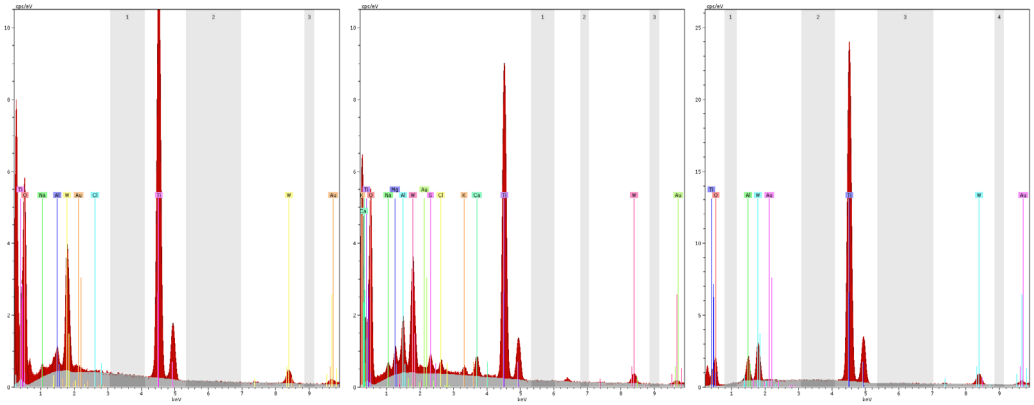

Figure S12. SEM-EDX spectra of the Au/TiO_2/WO_3-NWH—HA heterostructures.

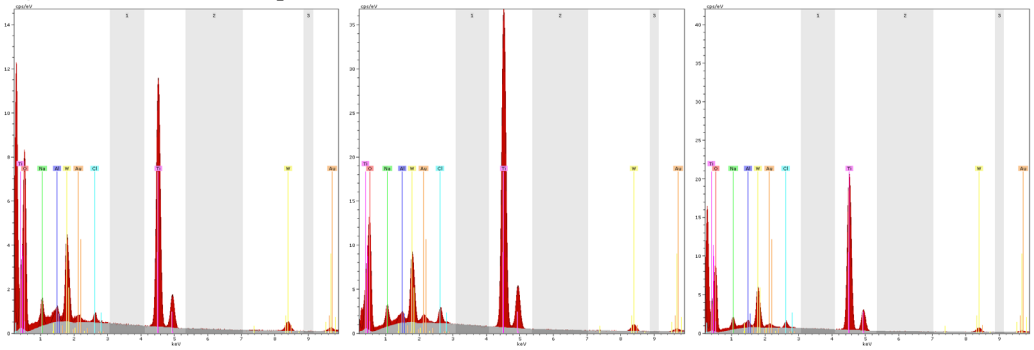

Figure S13. SEM-EDX spectra of the Au/TiO_2/WO_3-NWH—TA heterostructures.

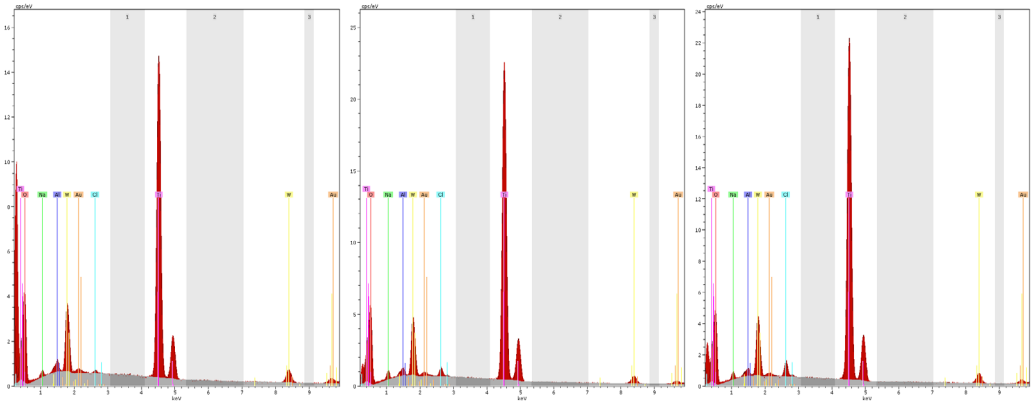

Figure S14. SEM-EDX spectra of the Au/TiO_2/WO_3-AMT—HA heterostructures.

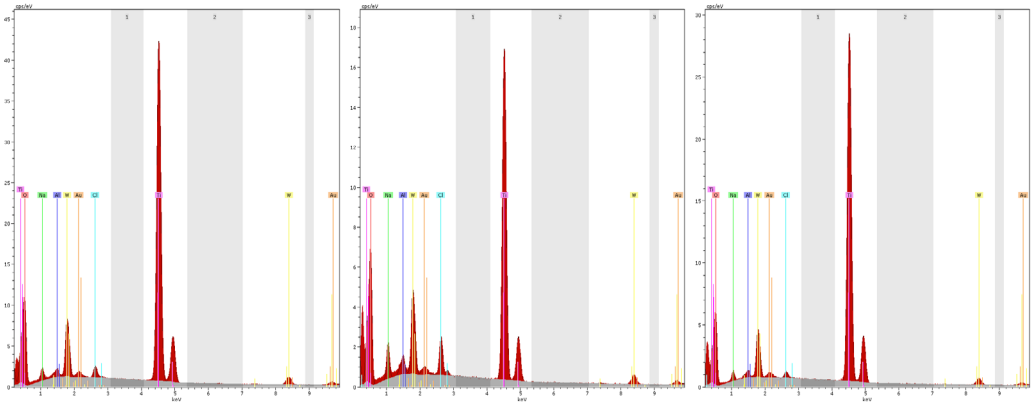

Figure S15. SEM-EDX spectra of the Au/TiO_2/WO_3-AMT—TA heterostructures.

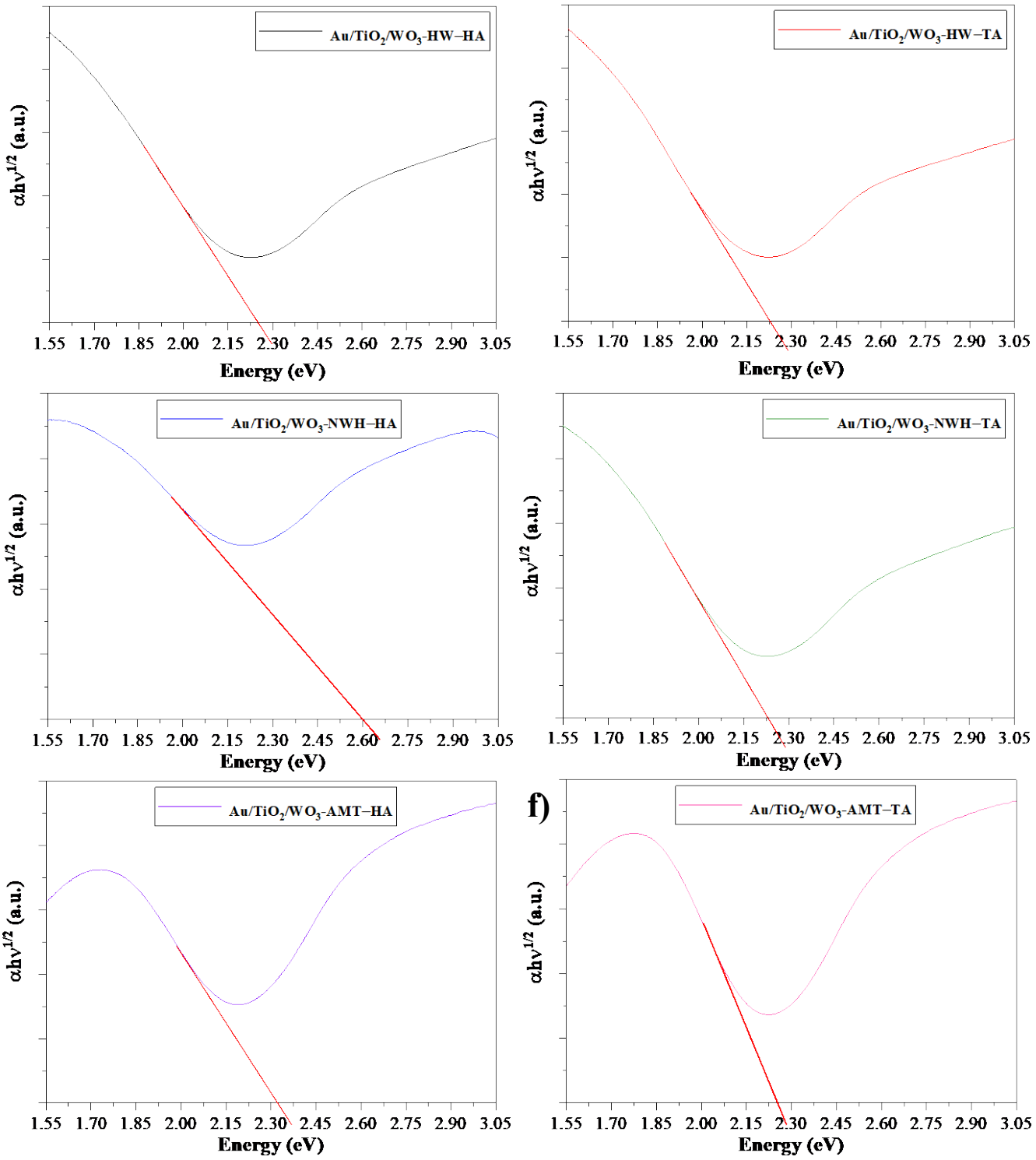

Figure S16. Individual Tauc plots of the Au/TiO_2/WO_3 heterostructures: a) Au/TiO_2/WO_3-HW–HA; b) Au/TiO_2/WO_3-HW–TA; c) Au/TiO_2/WO_3-NWH–HA; d) Au/TiO_2/WO_3-NWH–TA, e) Au/TiO_2/WO_3-AMT–HA; and f) Au/TiO_2/WO_3-AMT–TA.

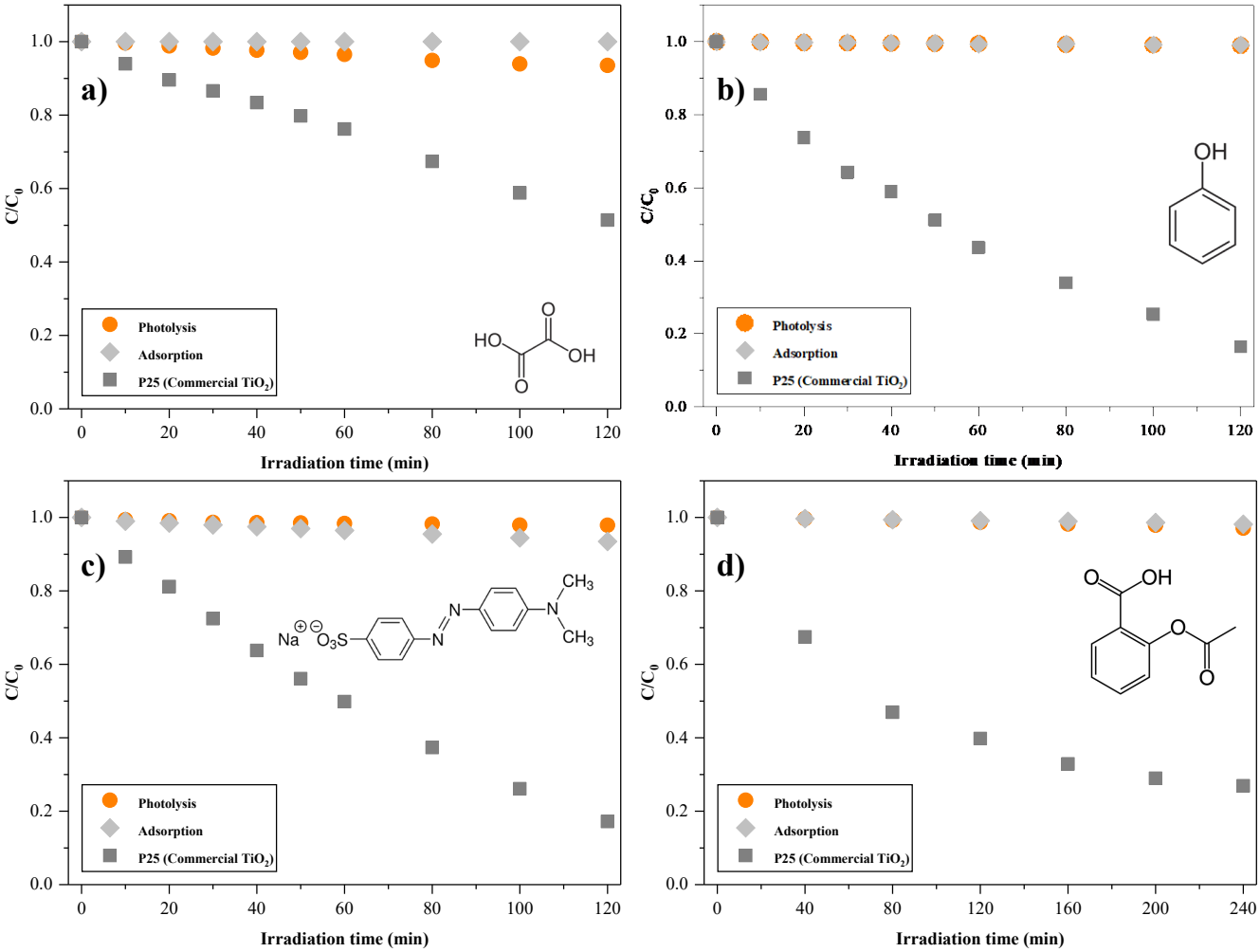

Figure S17. Photolysis, adsorption, and photocatalytic activity measurements of commercial TiO_2 for each model pollutant: a) oxalic acid; b) phenol; c) methyl orange; d) aspirin.

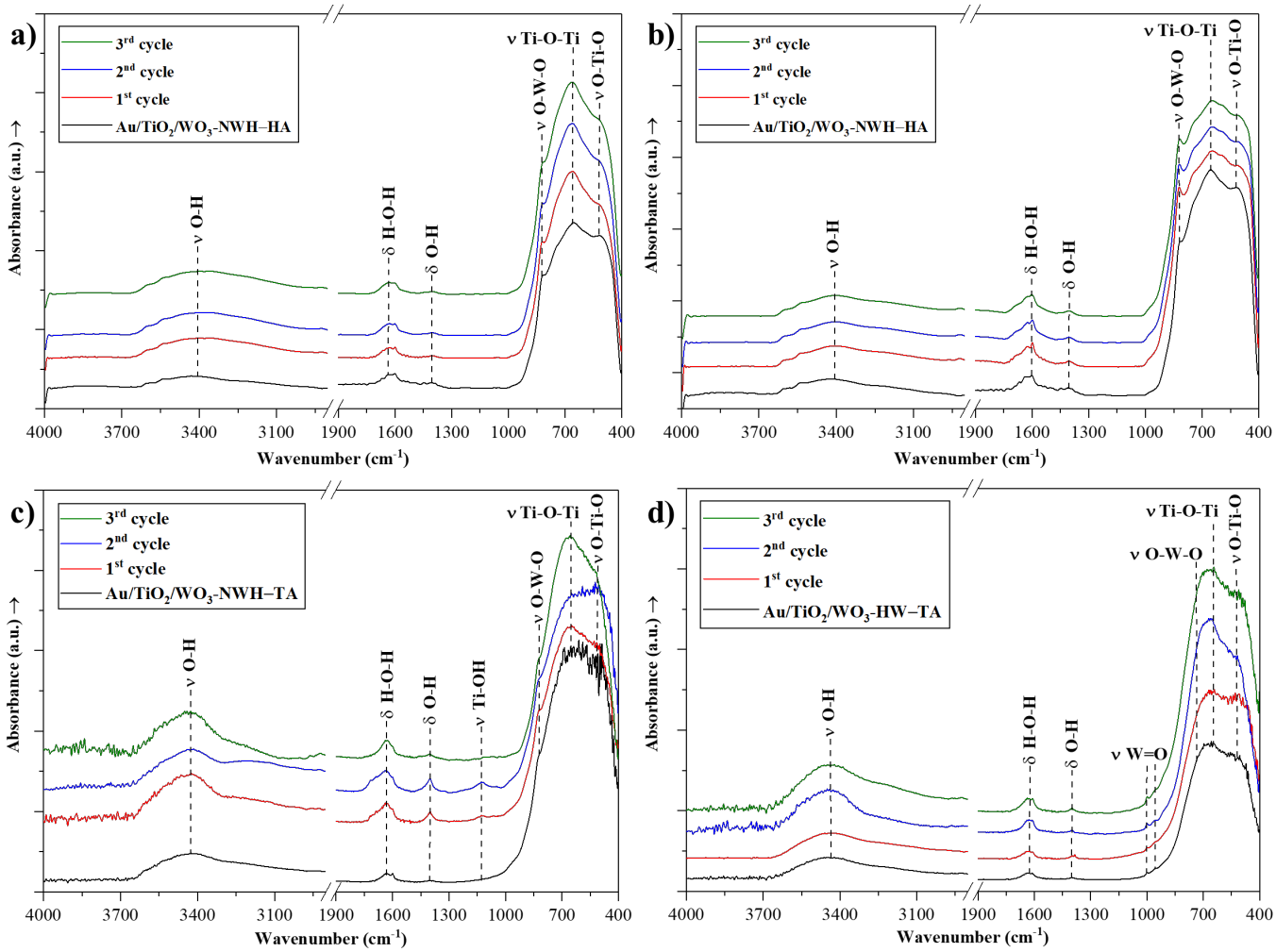

Figure S18. Stability of the Au/TiO_2/WO_3 heterostructures after several cycles of recyclability (after OA removal a); after PHE removal b); after MO removal c); and after ASP removal d).

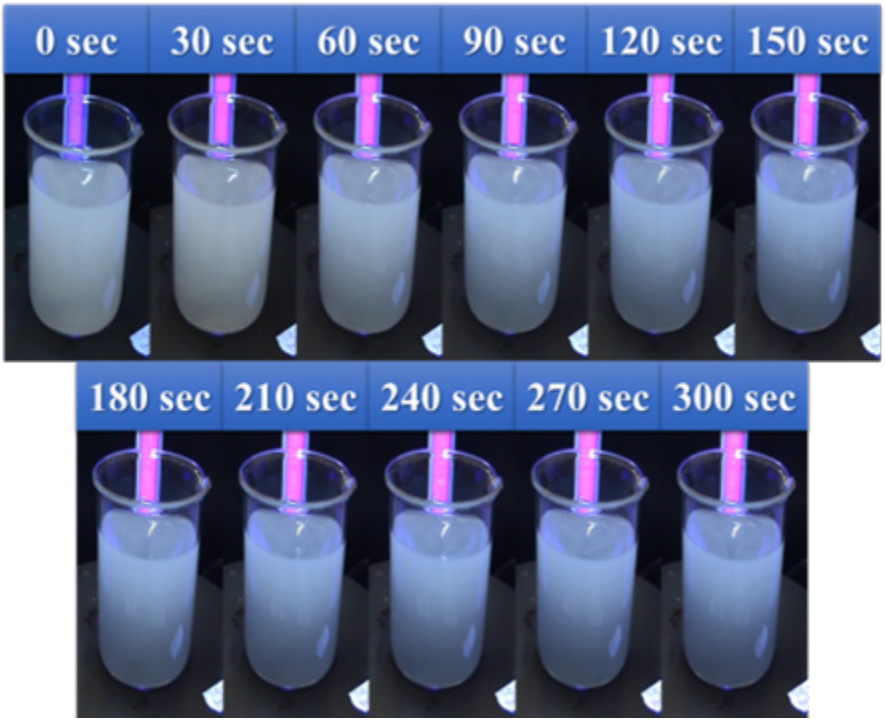

Figure S19. Blue colorization of the OA suspension.

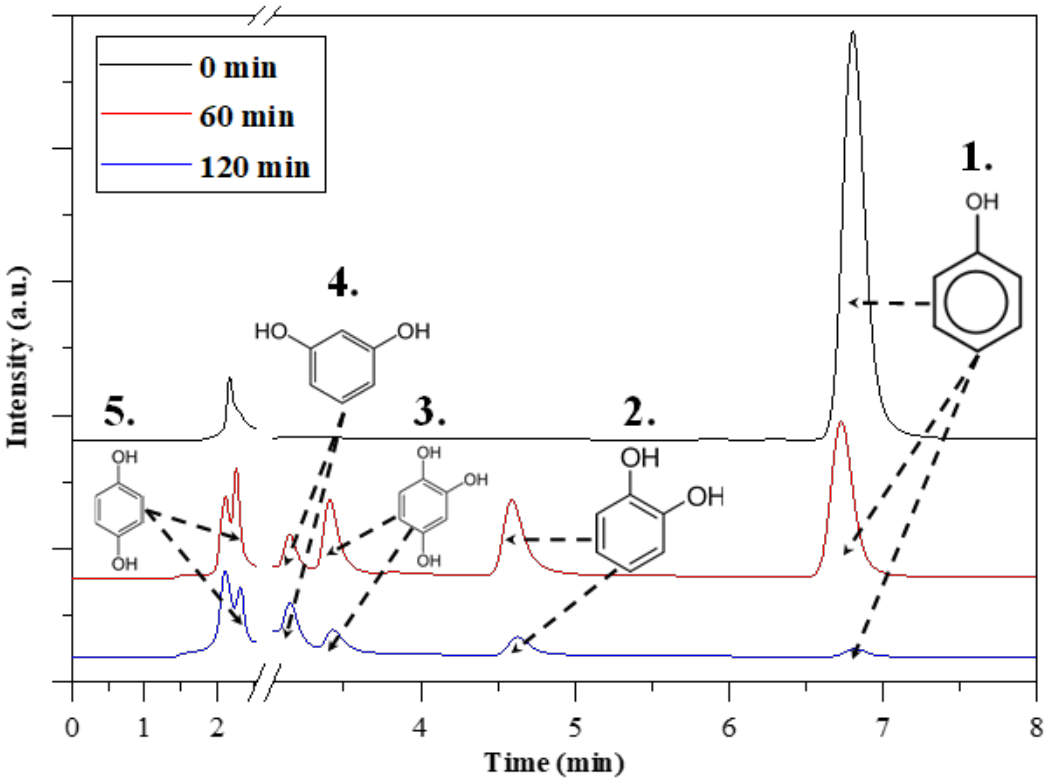

Figure S20. Chromatograms of phenol at initial concentration and after 60 and 120 minutes of UV light exposure.

Table S1. Summary of the Au/TiO_2/WO_3 heterostructures' photocatalytic activity under UV and Vis light irradiation.

Sample	Aspirin conversion (%)	Methyl orange conversion (%)	Phenol conversion (%)	Oxalic acid conversion (%)
Au/TiO_2/WO_3-HW−HA	72.7	74.9	88.3	67.1
Au/TiO_2/WO_3-HW−TA	82.1	56.9	96.8	95.9
Au/TiO_2/WO_3-NWH−HA	44.0	90.1	99.0	96.6
Au/TiO_2/WO_3-NWH−TA	64.5	97.9	97.9	62.6
Au/TiO_2/WO_3-AMT−HA	69.1	48.8	96.3	41.9
Au/TiO_2/WO_3-AMT−TA	81.6	61.0	98.2	61.9
P25 (Commercial TiO_2)	73.1	82.8	83.5	48.6